Journal Name

ARTICLE

Systematic investigation on synthesis and light-absorption broadening of a novel diketopyrrolopyrrole conjugated polymer of low and high molecular weight with thermo-labile groups

Long Yang,[a] Yuyan Yu,[a] Yulong Gong,[b] Jiarong Li,[a] Feijie Ge,[a] Long Jiang,[a,*] Fang Gao,[b] and Yi Dan[a,*]

To strengthen the π-π stacking interaction of conjugated polymer chains and study the absorption broadening effect, a narrow band-gap copolymer with high (DPP-Car-Boc-H) and low (DPP-Car-Boc-L) molecular weight, comprising alkyl substituted diketopyrrolopyrrole (DPP) and t-butoxycarbonyl (t-Boc)-protected carbazole (Car-Boc) units, is designed and synthesized . The absorbing broadening is investigated on the basis of molecular weight, solution and solid state, solution temperature and nonsolvent effect. FTIR analysis confirmed the decomposition of t-butoxycarbonyl protecting groups after thermal annealing treatment. It is found that the remove of thermo-labile groups (t-Boc) at 180℃ and the liberation of active NH groups further broaden the light-absorbing spectra in thin film due to the intensified π-π stacking interaction between polymer chains which are verified through TGA, SEM and XRD. After thermal annealing, SEM images exhibited cubic crystals spreading uniformly and the increased order degree of aggregation was verified further. Additionally, the impact of electronic structure change on the photo-response broadening effect is excluded by the Gaussian molecular simulation. This work provides a viable approach and convincing evidences for the thermal fabrication to strengthen the conjugated polymer chains stacking through the large π-delocalized plane and obtain broad absorption property for the use in photoelectric devices.

Introduction

Spectral sensitization of narrow band-gap semiconductors in photoelectric devices is an attractive approach for conversion of the visible part of solar energy into electricity in which the charge and energy transfer efficiency is a major issue.[1] Interchain interactions impacting charge delocalization are, therefore, crucial in understanding the charge transport in polymer solar cells (PSC) devices, as well as field-effect transistors (FET) and polymer light-emitting diode (PLED).[2] The orientation and packing of semiconducting polymer chains at film crucially affects the interaction, charge injection and transport between the conjugated polymer chains [3] and relatively photophysical properties could effectively reflect intermolecular interactions within conjugated polymer condensed phases. Thus it is of great value to study the relationship between polymer aggregates and absorbing change, especial the absorbing broadening effect in the solid film of the conjugated polymers.

Diketopyrrolopyrrole (DPP) based polymers as the most commonly reported materials, is widely researched in PSC, FET, PLED and etc., due to their versatile photophysical and electronic properties obtained by coupling various aromatic and heteroaromatic moieties.[4] The DPP core with electron deficient nature exhibits a planar conjugated bicyclic structure and acts as acceptor unit, which leads to strong π-π interactions. Besides, the two thiophene units adjacent to the core can expand the π delocalization and alleviate their steric repulsions with DPP to maintain high coplanarity of the polymer backbone, which is essential for achieving efficient charge transport properties and low band gaps.[5] It is well known that compact interaction of polymer chains through π-π stacking of the conjugated plane can facilitate the charge or electron transfer in the DPP-based photoelectric devices. Thus, the cognition and relationship of π-π stacking, aggregation and orientation and photophysical property of conjugated polymer chains deserves noteworthy attention and research.[6]

Not like small molecules, in most cases the huge chain and molecular weight can prevent polymers to pack compactly through self-aggregation, electrostatic or hydrophobic interactions to form ordered structure and obtain wide spread π-π stacking degree, thus higher energetic hydrogen bonds would be a fine alternative. To strengthen the π-π stacking interaction of polymer chains, the treatment of the processed layers or films with heat is really a promising method through the cleavage of thermo-labile groups in the polymer chains due to the advantages of avoiding of solvents, low-

[a] State Key Laboratory of Polymer Materials Engineering of China (Sichuan University), Polymer Research Institute of Sichuan University, Chengdu 610065, China, e-mail: *Jianglong@scu.edu.cn, danyichenweiwei@163.com*
[b] College of Chemistry and Chemical Engineering, Chongqing University, Chongqing 400044, China

Polymer Chemistry Accepted Manuscript

temperature processing and controllability and tunability of structures.[7] Additionally, the π-π stacking interaction can be intensified through the hydrogen bonds which are located in or along the conjugated backbone.[8] Not perfectly, conjugated polymers with thermo-labile groups designed in the conjugated backbone and without causing the changes in the electronic properties of the polymers during the thermo-cleavage procedure have not been reported yet and the subsequent absorption broadening effect has not been studied specially and systematically. Additionally, the systematic progress in material engineering relies greatly in the fundamental understanding of the impact of structure (from atomic to microstructural and mesoscopic scales) on functional properties (i.e., mechanical, photophysical or charge carrier transfer characteristics).[9] In improving the previous work and making the most of functionality and planarity of carbazole, we design new version and simple synthetic route of an original DPP based polymer copolymerized with carbazole units bearing tert-butoxycarbonyl (t-Boc) protective groups (DPP-Car-Boc, see scheme 1). The t-Boc groups are known to undergo thermolysis at ~ 180 ℃and leave the unbound N-H group.[10] Therefore, they are advantageous to the low temperature hot-processing and formation of hydrogen-bonded network with a high chromophore density in thermo-annealing step. The functional groups, light-absorbing and aggregation behavior change before and after thermo-cleavage will be investigated. In focus, the π-π stacking induced absorption broadening effect is revealed systematically through the temperature dependant and nonsolvent induced aggregation absorption property, together with the photo-emission change in solution and solid state. Additionally, Gaussian molecular simulation is applied for the exclusion of molecular and electronic structure change effect on the light-absorbing broadening behaviour.

Experimental

Starting materials and sample preparation

2-thiophenecarbonitrile, 2-ethylhexyl bromide, 4-dimethylaminopyridine, tert-amyl alcohol and di-tert-butyl dicarbonate (Boc$_2$O) were purchased from Shanghai Titan Scientific Co., Ltd. Carbazole, methyl trioctyl ammonium chloride (Aliquat 336), n-BuLi (2.5M) in hexane, trimethylborate and Pd(PPh$_3$)$_4$ were obtained from Chengdu Astatech Trading Co., Ltd. All the starting materials and reagents were used without further purification except for THF, toluene and DMF with anhydrous treatment. Column chromatography was performed on silica gel (70-80 A, Qingdao Hailang).

The thin films on glass were obtained through dip-evaporation and natural levelling of the target polymers dissolved in chlorobenzene with a concentration of 1.0 mg/mL.

Instruments

^{1}H-NMR and ^{13}C-NMR spectra were recorded on a Bruker Avance Ⅱ -400MHz. UV / vis spectra were measured on a UV-

2300 spectrophotometer (Hitachi, Japan). Fluorescence spectra were recorded on an F4600 spectrometer (Hitachi, Japan) excited at 430 nm for both solution and thin film. SEM images were taken on Quanta-250 scanning electron microscope (American FEI Cooperation). MALDI-TOF-MS spectra were measured in chlorbenzene from Autoflex III (Bruker, U.S.), with 2,5-dihydroxybenzoic (DHB) and 2,6-dihydroxyacetophenone (DHAP) as matrix and sodium trifluoroacetate as ionizing agent. The molecular ground-state geometries were optimized using Becke's three parameter hybrid exchange-correlation (XC) functional B3LYP [11] and 6-31G (d, p) basis which were performed using Gaussian 03 software package [12]. X-ray diffraction (XRD) measurements were carried out with a DX-2500 spectrometer (Dandong, China). Fourier Transformation Infra-red Spectroscopy (FTIR) spectra were measured on a Nicolet IS10 spectrometer (Thermo Fisher Scientific, America). Gel permeation chromatography (GPC) analyses were carried out on a Shimadzu 20AD (Japan) instrument for the DPP polymers with low molecular weight, using THF as eluent and polystyrene standards as calibrants. Thermogravimetric analysis (TGA) measurements were performed on SDT Q600 analyzer under a nitrogen flow, heating from room temperature to 600 ℃, with a heating rate of 10 ℃ min^{-1}. The electrochemical measurements were carried out on the CorrTest workstation (Wuhan Corrtest instruments Co., LTD). The polymers were dissolved and cycled in dichloromethane (saturated with nitrogen) containing 0.1 M tetrabutylammonium hexa-fluorophosphate (TBAPF$_6$) as the electrolyte salt. Platinum wire was used as reference and counter electrodes. The voltage data are calculated for the standard calomel electrode (SCE). Scan rate: 100 mV s^{-1}, temperature: 25℃.
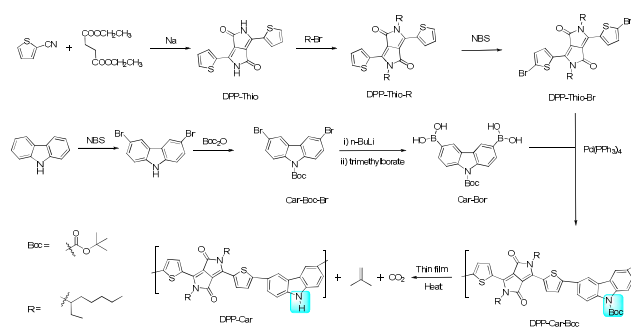
Synthesis

Scheme 1 Synthesis of the target DPP polymers.

DPP-Thio (3,6-bis(thiophen-2-yl)-2H,5H-pyrrolo[3,4-c]pyrrole-1,4-dione).

To a nitrogen-protected three-neck round-bottom flask equipped with a mechanical stirrer, a thermometer and a reflux condenser, were added tert-amyl alcohol (30 mL). The mixture was heated to 80 ℃ for 10 min before small peaces of sodium (0.8 g, 34.8 mmol) was added quickly. After heating to 115 ℃ for 30 min to make sodium dissolved completely, 2-thiophenenitrile (2.0 g, 18.4 mmol) was added. The stirring continued at 115 ℃ for 10 min. A mixture of diethyl succinate

(1.6 g, 9.2 mmol) in *tert*-amyl alcohol (10 mL) was added in the speed of 1 drops/2s with rapid stirring. The mixture was then stirred at 115 ℃ for a further 3 h. After cooling to room temperature, a mixture of methanol (80 mL) and con. HCl (5 mL) was added. The solid was filtered and washed with methanol (100 mL), water (100ml) and methanol (100 mL). Then the filter cake was dried at 40 ℃ under vacuum to give the product as maroon solid (2.2 g, yield = 79%). ^{1}H-NMR (*d*-DMSO, 400 MHz) 7.292-7.314 (2H, dd, *J1* = 4.8, *J2* = 4.0), 7.961-7.974 (2H, d, *J* = 5.2), 8.220-8.229 (2H, d, *J* = 3.6), 11.262 (2H, s).

DPP-Thio-R (2,5-di-(2-ethylhexyl)-3,6-bis(thiophen-2-yl)pyrrolo[3,4-c]pyrrolo-1,4-dione)

DPP-Thio (0.5 g, 1.7 mmol) was dissolved in anhydrous DMF (10 mL). Then to the solution was added NaH (0.2 g, 60% w/w in kerosene) and catalytic amount of KI. After heating under nitrogen at 60℃ for 30 min, 1-bromo-2-ethylhexane (0.7 g, 3.6 mmol) was added and the reaction mixture stirred at 80 ℃ for a further 12 h. The reaction mixture was allowed to cool to room temperature then it was poured into ice water (50mL) and the resulting suspension was extracted with CH_2Cl_2 and recrystallized from MeOH to give a dark red solid (0.26 g, yield = 40%). ^{1}H-NMR(CDCl$_3$, 400 MHz) 0.834-0.895 (12H, m), 1.225-1.380 (16H, m), 1.848-1.878 (2H, m), 4.010-4.043 (4H, m) 7.268-7.280 (2H, m), 7.616-7.631 (2H, m), 8.877-8.889 (2H, m).

DPP-Thio-Br (3,6-bis(5-bromothiophen-2-yl)-2,5-di-(2-ethylhexyl)pyrrolo[3,4-c]pyrrolo-1,4-dione)

N-bromosuccinimide (3.5 g, 19.6 mmol) was added to a solution of DPP-Thio-R (5.0 g, 9.5 mmol) in chloroform (100mL) at room temperature, wrapped in aluminum foil to exclude light. The reaction was monitored by TLC and stopped as soon as no more mono-brominated species was observed by TLC (approximately 50 min). Under stirring methanol (200 mL) was added slowly to the mixture followed by stirring in an ice bath overnight. The solid was filtered, washed with methanol (2 × 200 mL) and dried under vacuum to give the product as a dark red solid (4.5 g, yield = 70%). ^{1}H-NMR (CDCl$_3$, 400 MHz) 0.848-0.904 (12H, m), 1.253-1.373(16H, m), 1.805-1.869 (2H, m), 3.880-3.990 (4H, m), 7.221-7.231 (2H, d, *J* = 4.0), 8.641-8.651 (2H, d, *J* = 4.0); ^{13}C-NMR (CDCl$_3$, 400 MHz) 10.494 (2C), 14.034 (2C), 23.056 (2C), 23.605 (2C), 28.360 (2C), 30.219 (2C), 39.144 (2C), 46.052 (2C), 108.057 (2C), 119.026 (2C), 131.200 (2C), 131.494 (2C), 135.390 (2C), 139.439 (2C), 161.438 (2C).

Car-Boc-Br (tert-butyl-3,6-dibromo-9H-carbazole-9-carboxylate)

Carbazole (5.0 g, 30 mmol) was dissolved in CH_2Cl_2 (250 mL). *N*-Bromosuccinimide (NBS) (10.7 g, 60 mmol) in DMF (50 mL) was then added slowly. The reaction mixture was stirred for 5h at room temperature in the absence of light under argon atmosphere. To the mixture was added water (300 mL). The organic layer was washed with brine (3 × 150 mL), dried over Na$_2$SO$_4$, filtered, evaporated and recrystallized from EtOH to give 3,6-dibromo-9H-carbazole as light gray solid (7.2 g, yield = 74.2%) which was used directly in the next step.

To the solution of 3,6-dibromo-9H-carbazole (5.0 g, 15.4 mmol) in CH_3CN (50 mL) under nitrogen, di-tert-butyldicarbonate (6.7 g, 30.7 mmol) was added at room temperature. After stirring for 10 min at room temperature, 4-dimethylaminopyridine (1.9 g, 15.5 mmol) was added slowly. After the reaction was finished (2h), the mixture was poured into water (200mL). The solid was filtered and washed with MeOH. After filtration through a flash column with CH_2Cl_2 and hexaneand, crystallization in MeOH and evaporating under reduced pressure, a white solid (4.7 g, yield = 73%) was obtained. ^{1}H-NMR (CDCl$_3$, 400 MHz) 1.750(9H, s), 7.563-7.590 (2H, dd, *J1* = 8.8, *J2* = 2), 8.040-8.045 (2H, d, *J* = 2) 8.151-8.174 (2H, d, *J* = 9.2).

Car-Bor (9-(tert-butoxycarbonyl)-9H-carbazole-3,6-diyldiboronic acid)

Car-Boc-Br (2.0 g, 4.7 mmol) was dissolved in 80mL of dried THF and n-BuLi (2.5M in hexane, 4.2 mL, 10.4 mmol) was added by syringe at -80 ℃ under the protection of Ar flow. Then the mixture was kept stirring for 1h before trimethylborate (1.2 mL, 10.4 mmol) was added and the temperature of reaction system was ensured in the range of -78 ℃ and -85 ℃. 30 min later, the resulting mixture was heated to -30 ℃ and 2N HCl aqueous solution was added slowly to make sure the pH was 2~3. After 30 min of stirring, the reaction mixture was abstracted with CH_2Cl_2. The combined organic layers were washed with brine, dried by anhydrous NaSO$_4$, filtered and then evaporated. The crude product was purified by chromotography with ethyl acetate-hexane (1: 1) as the eluent and then was further recrystallized in the mixture of MeOH and THF to give the final product as a white solid (1.3 g, yield = 78%). ^{1}H-NMR (d-DMSO, 400 MHz) 1.731 (9H, s), 7.944–7.965 (2H, d, *J* = 8.4), 8.151(4H, s), 8.184-8.205 (2H, d, *J* = 8.4), 8.594 (2H, s); ^{1}H-NMR (d-DMSO and D$_2$O, 400 MHz) 1.756 (9H, s), 7.980–7.985 (2H, s), 8.235-8.245 (2H, s), 8.586 (2H, s).

DPP-Car-Boc (DPP-Car-Boc-H and DPP-Car-Boc-L)

DPP-Thio-Br (0.50 g, 0.73 mmol) was dissolved in anhydrous toluene (25 ml) and the solution was stirred under Ar atmosphere for 10 min at 30 ℃. Then to the mixture, Pd(PPh$_3$)$_4$ (0.08 g, 10 mol %), a solution of Car-Bor (0.26 g, 0.73 mmol) in anhydrous THF (5mL), catalytic amount of Aliquat 336 and K$_2$CO$_3$ aqueous solution (2 M, 0.7 mL) were added subsequently. The polymerization was carried out at 80 ℃ for 30 h under argon protection. Next, the mixture was cooled to ambient temperature and dropped into the mixture of methanol (100 mL) and water (20 mL). The raw product was filtered off and subjected to subsequent Soxhlet extractions with methanol, hexane, acetone, chloroform and chlorbenzene. DPP-Car-Boc-L and DPP-Car-Boc-H was obtained from chloroform and chlorbenzene extraction subsequently. **DPP-Car-Boc-L** (0.1 g, dark purple); M$_w$/M$_n$ (GPC) = 3320/2818; ^{1}H-NMR (CDCl$_3$, 400 MHz) 0.899 (12H, s), 1.258-1.397 (16H, m), 1.626 (2H, s), 1.737-1.819 (9H, m), 4.077 (4H, s), 7.447–7.715 (5H, m), 8.128-8.227(3H, m), 8.901-8.980 (2H, m); **DPP-Car-Boc-H** (0.2 g, dark purple); ^{1}H-NMR (d-chlorbenzene, 400

MHz) 1.175 (12H), 1.344-1.402 (16H), 1.900 (2H), 2.023-2.070 (9H), 4.584 (4H), 7.076-7.009 (2H), 7.216 (1H), 7.147 (2H), 7.628 (1H), 7.932–7.988 (2H), 8.108-8.122(2H).

DPP-Car (DPP-Car-H and DPP-Car-L)

The thin films precursor of DPP-Car-Boc on glass were annealed in an oven at 150 ℃ and 180 ℃ for 30 min respectively to obtain the thin films of DPP-Car (DPP-Car-H and DPP-Car-L) which are characterized by FTIR and discussed below. The ^{1}H-NMR, ^{13}C-NMR charts, MALDI-TOF-MS and TGA results are attached in Electronic Supplementary Information (ESI).

Results and Discussion

Synthesis and characterization

The synthetic route to the thermo-cleavable DPP polymers is outlined in Scheme 1. Starting from 2-cyanothiophene, a condensation reaction was performed to get DPP-Thio; this step was then followed by an alkylation reaction with 1-bromo-2-ethylhexane and a dibromination reaction with NBS to yield DPP building block (DPP-Thio-Br). The carbazole building block (Car-Bor) was successfully obtained from boronation of Car-Boc-Br and characterized by ^{1}H-NMR in both D_2O and d-DMSO. The chemical shift (ESI Figure S6 and S7) of hydroxyl groups of boric acid appeared at 8.151 ppm as a single peak, and it disappeared when D_2O was added to the solution due to proton exchange. As shown in Scheme 1, the two comonomers were copolymerized through versatile Suzuki cross-coupling polymerization with $Pd(PPh_3)_4$ as the catalyst to afford DPP-Car-Boc in good yield. In the soxhlet extraction procedure, $CHCl_3$ was used to extract the DPP polymer with low molecular weight to give DPP-Car-Boc-L, and due to the low solubility of DPP polymer with high molecular weight, chlorobenzene was used to extract DPP-Car-Boc-H which was characterized with ^{1}H-NMR in chlorobenzene (ESI Figure S10), FTIR (Figure 1) and MALDI-TOF-MS spectra (ESI Figure 11 and 12). As shown in MS spectra, the molecular weight of DPP-Car-Boc-H is higher than that of DPP-Car-Boc-L.
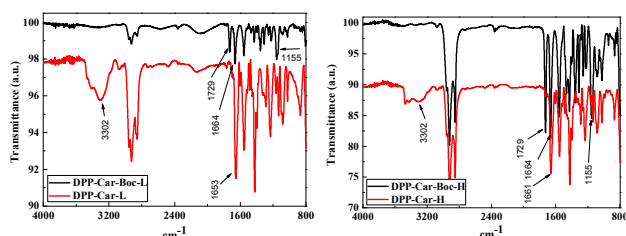

Figure 1 FTIR charts of DPP polymers in thin film before (black curves) and after (red curves) annealing.

To study the absorption broadening and aggregation effect in situ, thin films were obtained through dip-evaporation method, and the cleavage of DPP-Car-Boc-H and DPP-Car-Boc-L was carried out in thin film on glass to give DPP-Car-H and DPP-Car-L, respectively. FTIR is a very convenient analytic characterization technique to indicate whether the polymer

consist of carbonates cleaved functionalities on the backbone (i.e., amino group). Figure 1 shows FTIR spectra before (black) and after (red) the cleavage, which clearly show the split-off of the t-butyloxy carbonyl group (Boc). The carbonates in DPP-Car-Boc-H and DPP-Car-Boc-L give rise to a strong band at 1729 cm^{-1} due to the N atom in carbazole, which can be assigned to the carbonyl stretching mode. After the cleavage, the carbonyl band disappears completely and the liberated amino functionality (3302 cm^{-1}) of DPP-Car-H and DPP-Car-L can be detected. Scheme 1 shows the probable decomposition mode after heating at 180 ℃ for 30 min.[7a,8] Additionally, the disappearance of C-O asymmetry stretching vibration (1155 cm^{-1}) verifies the cleavage of the t-butyloxy carbonyl group from the backbone again. It is found that the $\upsilon_{C=O}$ (amide) has shifted from 1664 cm^{-1} to lower energies 1661cm^{-1} (by ~ 3 cm^{-1}) for DPP-Boc-Car-H and from 1664 cm^{-1} to lower energies 1653cm^{-1} (by ~ 11 cm^{-1}) for DPP-Boc-Car-L after thermal treatment, which is indicative of the hydrogen bonding (C=O······H-N) along the polymer backbone.[8]

The relative (in)stability of the DPP-Car-Boc-H and DPP-Car-Boc-L was investigated by thermogravimetric analysis (TGA) in the temperature range up to 300 °C (ESI Figure S16 and S17). Combining the FTIR results, a conclusion could be made that the t-butyloxy carbonyl group could decompose and remove effectively and completely after heating at 180 ℃ for 30 min.

Absorption broadening

Solution- and solid-state absorption spectra of DPP-Car-Boc-H and DPP-Car-Boc-L prepared in chlorobenzene are provided in Figure 2. The first absorption band stands between 450 nm to 700 nm, originating from a localized intramolecular charge transfer (ICT) between the donor (carbazole) and acceptor (DPP) segments in push–pull type conjugated molecules [13] which will be illustrated by molecule simulation below. The similar absorption peaks (λ_{max}) in both solution and solid state indicate that the absorption π-π* transition of the two polymers comes from the same frontier orbitals and they have
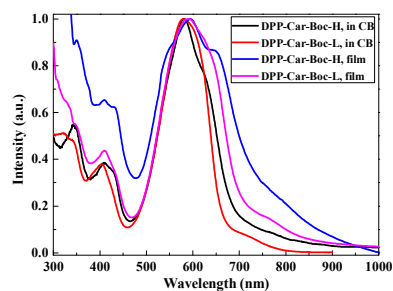

Figure 2 The absorption property of DPP polymers in chlorbenzene (CB, 0.01mg/ml) and thin film.

similar molecular structure except for the molecular weight. Compared with DPP-Car-Boc-L, the slight red-shift of onset absorption (λ_{onset}) comes from the increased degree of conjugation for DPP-Car-Boc-H as the extended π-conjugation is helpful to improve photo-response range of the DPP polymers.[14] In the solid state, both DPP-Car-Boc-H and DPP-

Car-Boc-L exhibit larger λ_{onset} (762 nm and 710 nm, respectively) than that in solution (697 nm and 673 nm, respectively) as shown in Table 1. DPP-Car-Boc-H shows a significant red-shift (~65 nm) of absorption onset, which can be attributed to solid state packing effect, [15] whereas for DPP-Car-Boc-L, the increasing range is much smaller (~47 nm). The remarkable shoulder peak around 762 nm for DPP-Car-Boc-H in film also indicates the more ordered packing of conjugated

polymer chains than that of other samples.[16] The larger the molecular weight is, the more apparent the absorption broadening is, and the same effect was also reported for Si-PDTBT system.[17] The obvious absorption broadening effect in the solid state indicates stronger ICT between carbazole and DPP segments together with intimate chain contacts compared with that in the solution state.

Table 1 Optical and electrochemical data of the synthesized DPP polymers

Polymers	$\lambda_{max}^{a} / \lambda_{onset}^{a}$ (nm)	$E_g^{a,opt}$ (eV)	$\lambda_{max}^{b} / \lambda_{onset}^{b}$ (nm)	$E_g^{b,opt}$ (eV)	λ_{max}^{a} [c] (nm)	λ_{max}^{b} [c] (nm)	$E_{onset(Red)}$ (V)/ LUMO (eV)	$E_{onset(Ox)}$ (V)/ HOMO (eV)	E_g^{CV} (eV) [d]
DPP-Car-Boc-H	581/697	1.78	594, 647/762	1.63	645/705	646/701	/	/	/
DPP-Car-H	588/696	1.78	607, 656/772	1.61	656/714	/	/	/	/
DPP-Car-Boc-L	582/673	1.84	590/710	1.75	645/701	645/698	-1.33/-3.07	0.58/-4.98	1.91
DPP-Car-L	586/675	1.84	607/751	1.65	652/709	/	-1.32/-3.08	0.58/-4.98	1.90

[a] Measured in solution. [b] Measured in film. [c] Emission. [d] E_g^{CV} electrochemical gap was calculated according to the following equation: $E_{HOMO} = - (E_{onset(Ox)} + 4.4)$, $E_{LUMO} = - (E_{onset(red)} + 4.4)$ [18]
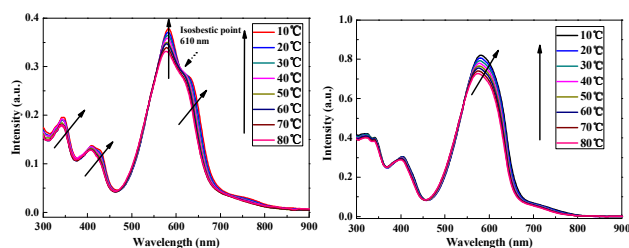

Figure 3 The temperature-dependant absorption properties of DPP-Car-Boc-H (Left) and DPP-Car-Boc-L (Right) in chlorobenzene (CB) solution (0.01mg/ml).

To study the movement and interaction of molecule chains in depth, the temperature-dependant absorption spectra of the conjugated polymers with low concentration (0.01mg/ml) were measured (Figure 3). For both DPP polymers with high and low molecular weight, upon the decrease of solution temperature the absorption peak shows red-shifted and photo-response broadening causing the increased onset (λ_{onset}) of absorption. The absorption behavior confirms the existence of polymer chains aggregates in solution.[19] The absorption maximum (λ_{max}) are fitted in linear formula against temperature as shown in ESI (Figure S13). The good degree of fit verifies that the molecular movement and stacking depend greatly on the temperature and the absorption broadening originates from the more compact interaction of conjugated polymer chains. Similar behavior could also be found for the thermo-treated samples DPP-Car-H and DPP-Car-L (Figure S14 and S15). This thermo-induced transition of absorption suggests that the polymer has a strong propensity for π-stacking.[20] When the temperature decreases the capability of molecular movement is restricted and thus the planar degree of conjugated chains and π-π stacking are intensified subsequently. Similar spectral changes have been observed upon cooling solutions of neutral poly-(3-alkylthiophenes) and the well-resolved red-shifted spectra obtained upon cooling correspond to π-stacked aggregated chain segments, which

can originate from both inter- and intrachain stacking interactions.[21] Noticeable, for DPP-Car-Boc-H the appearance of isosbestic point at 610 nm further indicates the interaction of polymer chains and the formation of aggregates.[20,22] Thus a conclusion can be made that the absorption broadening effect comes from the stronger ICT effect which is caused by much closer polymer chains packing and interaction.

Nonsolvents could also induce molecules to aggregate, so the absorption change of the conjugated polymers was recorded in chlorobenzene solution when MeOH was added as the nonsolvent. As shown in Figure 4, the absorption coefficient between 300-700 nm band decreases as the fraction of MeOH in chlorobenzene increases whereas the coefficient of longer absorbing band (880-1100 nm) increase obviously. Additionally, it is well marked that the absorbance of 880-1100 nm band of DPP-Car-Boc-H with higher molecular
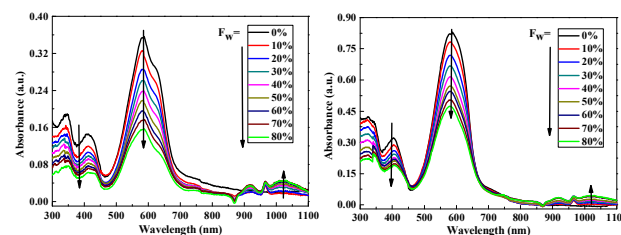

Figure 4 Absorption property of DPP-Car-Boc-H (left) and DPP-Car-Boc-L (right) in CB-MeOH mixed solvents (F_w = the fraction of MeOH).

weight increases more dramatically than that of DPP-Car-Boc-L, which might be caused by the larger molecular chain and π-conjugated degree . All these observations indicate that the DPP polymers contain strong interactions due to the conjugated π planes between polymer chains even in solution state.[23]
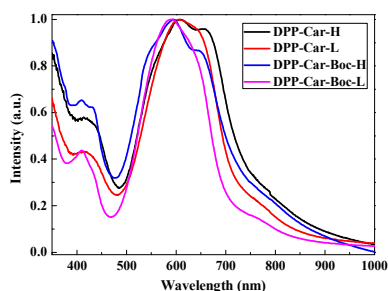
Figure 5. The absorption property of DPP polymers before and after thermo-treatment in thin film.

To study the light-absorbing change of the conjugated polymers with and without thermal-labile groups and the thermal annealing promoted the polymer aggregation, the light-absorbing property and aggregation characteristics of film samples in situ were examined on glass by UV-vis spectrometer, SEM and XRD. Much broader aggregate-type photo-response was observed in the DPP-Car-H and DPP-Car-Boc-L than in the DPP-Car-Boc-H and DPP-Car-L, respectively. After thermal annealing, the absorption maximum red-shifts 13 nm and 17 nm for DPP-Car-Boc-H and DPP-Car-Boc-L, respectively. The onset of absorption is also red-shifted greatly from 762 nm to 772 nm (corresponding to 1.63 eV→1.61 eV) for DPP-Car-Boc-H and from 710 nm to 751 nm (corresponding to 1.75 eV→1.65 eV) for DPP-Car-Boc-L. Noticeable, the red-shift degree of DPP-Car-Boc-L is larger than that of DPP-Car-Boc-H, indicating that the conjugated polymer with low molecular weight can move much more smoothly than that with high molecular weight and thus causes much stronger interchain packing and interactions between chains through π-π stacking and hydrogen bonds [8] which was also verified in the XRD measurements (Figure 10). Further the increasing absorbance of shoulder peak also represents the much more regular packing of molecular chains. This comparison reflects that the interchain interaction in the DPP polymer is strengthened by the replacement of t-butyloxy carbonyl protecting group with hydrogen in the carbazole units, as is intended, and the light-absorbing effect is obtained for the film sample together with the enhanced packing of conjugated chains.
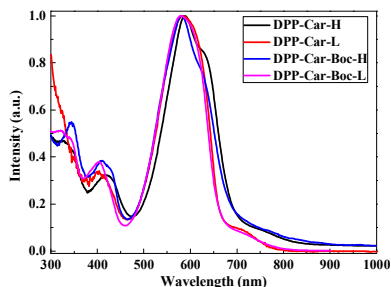

Figure 6. The solution absorption property of DPP polymers before and after thermo-treatment in chlorbenzene solution.

To exclude the impact of the molecular structure change on the electronic transition, the absorption property change of the conjugated polymers were recorded in chlorbenzene before and after thermal annealing, and further the molecular structures were optimized by Gaussian package with and without protecting group (t-Boc) which will be discussed in the molecule simulation section. As shown in Figure 6 and Table 1, DPP-Car-Boc-H and DPP-Car-H exhibits the absorption peak at 581 nm and 588 nm with the onset at 697 nm and 696 nm (corresponding to the band gap of 1.78 eV and 1.78 eV), respectively. The similar results and same conclusion can be found for DPP-Car-Boc-L and DPP-Car-L. In summary, the absorbing spectra stay almost unchanged for DPP-Car-Boc-L and DPP-Car-L, DPP-Car-Boc-H and DPP-Car-H respectively. This reveals that the replacement of the t-butyloxy carbonyl on N atom of carbazole unit with H atom does not change the electronic structure of the backbone of the polymers as both the absorption of λ_{onset} and λ_{max} stay almost unchaged [24] which will be further verified below in molecule simulation. Thus a conclusion can be drawn that the tremendous broadening effect of the two conjugated polymers in thin film before and after thermal annealing is caused by the intensified ICT due to strengthened interaction of polymer chains, not induced by the electronic structure change of the polymer molecular chains.
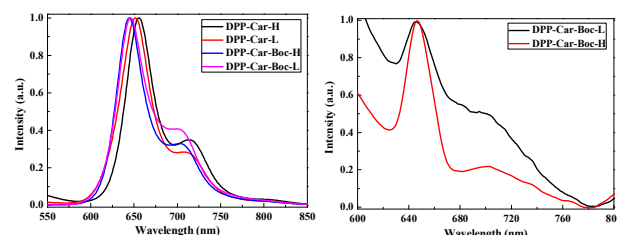
Photo-emission

Figure 7. The emission property of DPP-Car and DPP-Car-Boc in solution (left) and thin film (right).

The emission spectra for the DPP-based polymers in both solution and solid state are shown in Figure 7. As shown, the red-emissive peaks (about 600-770 nm) are highly similar. For DPP-Car-H and DPP-Car-L thin film sample, the emissive peaks are almost hardly detective and the photo-emission can not be detected. These suggest the sufficient fluorescence quenching because of the donor-acceptor architecture, strong intermolecular interactions and associated lower energy states (excimers, etc).[25] Strong π-π stacking typically leads to a non-emitting crystal phase as discussed in aggregation section, due to the forbidden low-excitonic transition.[26] Noticeably, in solution state the emission maximum of DPP-Car-H and DPP-Car-L are slightly red-shifted 11 nm and 7 nm respectively, compared with pre-thermo-annealing samples, but in thin film the emission maximum stay unchanged. We speculate that the red-shift of solution samples after thermal annealing is caused by intermolecular quench due to stronger interaction of polymer chains with hydrogen bonds. Stoke shifts of the four samples vary from 63 to 68 nm in solution and 40 to 55 nm in

thin film, respectively, which confirms that these polymers are rigid by nature with large conjugated plane.[27] Additionally, the excitation spectra of DPP-Car-Boc-L and DPP-Car-Boc-H in both chlorobenzene solution and thin film are provided in ESI (Figure S18-S20).
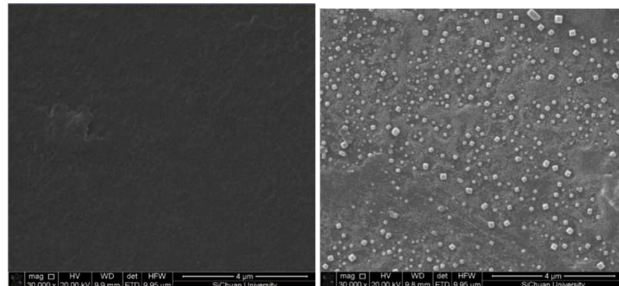
Aggregation behavior

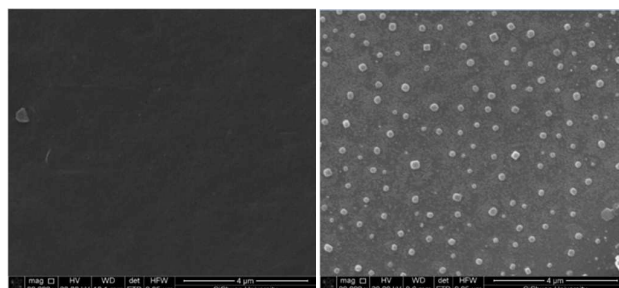Figure 8 SEM images of DPP-Car-Boc-H thin film on glass before (left) and after (right) annealing treatment.

Figure 9 SEM images of DPP-Car-Boc-L thin film on glass before (left) and after (right) annealing treatment.

SEM is a powerful and intuitive tool to study the aggregation behavior of the conjugated polymers deposited on glass. As shown in Figure 8 and 9, after thermal annealing, numbers of cube-like crystals with the size of 100-200 nm (DPP-Car-H) and 200-300 nm (DPP-Car-L) in length are clearly observed. During the thermal treating procedure, t-Boc group decomposes and gas is released.[7a, 28] The liberated N-H strengthens the intra-action and interaction of polymer chains through hydrogen bonds with C=O in the DPP unit. In the procedure of dip-evaporation by which the thin films are obtained, the rigid polymer chains aggregate in an amorphous form under the force of interchains π-π stacking which is confirmed by XRD in situ discussed below. As the thermo-annealing treatment is carried out below the melting point, the driving force can be ascribed to more intensified π-π stacking induced by intermolecular hydrogen bonds, thus the polymer chains are inclined to aggregate in much more condensed form to give little crystals spreading uniformly. Additionally, the crystal size of DPP-Car-L is larger than that of DPP-Car-H and this further explains the molecular chain movement during the annealing step because the length of molecular chains of DPP-Car-L is shorter than that of DPP-Car-H thus the former can move more smoothly than the latter. As formerly reported, perfect ordering and stretching of P3HT chains in a single crystal can lead to a significantly broad and different light absorption,[29]

consequently the crystal induced light-absorption broadening is much more reasonable.

To further reveal the aggregation and stacking behavior of the conjugated polymer chains, XRD measurement of thin film on glass were carried out directly. Broad peaks in the region of 2θ = 15-40° were observed which represent the (010) planes. Interestingly, as indicated in Figure 10, no clear peak was found in lamellar packing, indicating a formation of amorphous solid state structure exhibiting short-range order,[24b] whereas the feature of π-π stacking (d 010) is pronounced
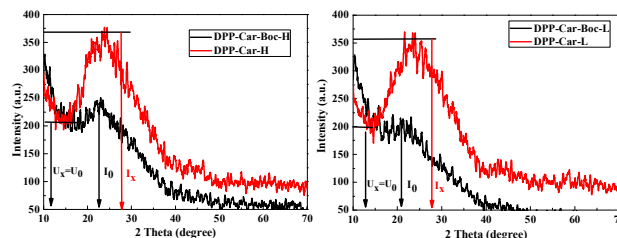

Figure 10 XRD results of thin films of the conjugated polymers on glass before (black) and after (red) annealing treatment.

in the film sample, which is also observed in PBDT-based polymers.[30] For the thin film of both DPP-Car-Boc-H and DPP-Car-Boc-L, without annealing, the peaks around 22.0° correspond to their π-π distances of about 0.39 nm, and in contrast after annealing treatment the peaks shift slightly to around 23.8° which corresponds to π-π distances of 0.37 nm. The π-π stacking distance in the above-mentioned copolymers is larger than that (0.356 nm) of earlier reported thienylene–vinylene–thienylene (PDPP-TVT) alternating copolymers but quietly equivalent to other DPP copolymers.[31] This further verifies the increased interactions of polymer chains through π-π stacking as illustrated in the photo-absorbing section after the removal of t-butyloxy carbonyl protecting group.[32]

These planes originate from the co-facial π-π stacking distances of polymer chains and the intensified response signals reveal that after annealing the conjugated polymer chains aggregate in a larger degree due to the intermolecular hydrogen bonds. Additionally, the extent of orientation can be thought of as the order degree of macromolecule in amorphous polymers, and the order degree (X) is evaluated by the following formular [33]:

$$X = \frac{I_x}{U_x} \times \frac{U_0}{I_0} \times 100\% \tag{1}$$

U_0 and U_x denote the backgrounds of the samples before and after annealing whereas I_0 and I_x are integral intensities of diffraction lines of the samples before and after annealing, respectively. As shown in Figure 10, corresponding to the order degree (X) the values of DPP-Car-Boc-H and DPP-Car-Boc-L are 1.55 and 1.80, respectively, which indicates that the order degree of the two samples are both intensified after annealing treatment. Combining with the former results and analysis, we can draw a conclusion that the absorption broadening after thermo-annealing treatment originates from the hydrogen bonds induced-enhancement of conjugated plane packing in the form of π-π stacking.

Journal Name

ARTICLE

Table 2. The molecular structure and frontier orbitals data in ground state

Polymers	Dihedral angles (°)		HOMO	LUMO	Eg
	Car-Thio [a]	DPP-Thio [b]	(eV)	(eV)	(eV)
DPP-Car-Boc	22.3/20.1	27.2/26.1	-5.14	-2.59	2.55
DPP-Car	20.1/19.7	28.9/27.2	-4.94	-2.49	2.45

[a] The dihedral angles between carbazole plane and thiophene. [b] The dihedral angles between DPP plane and thiophene.
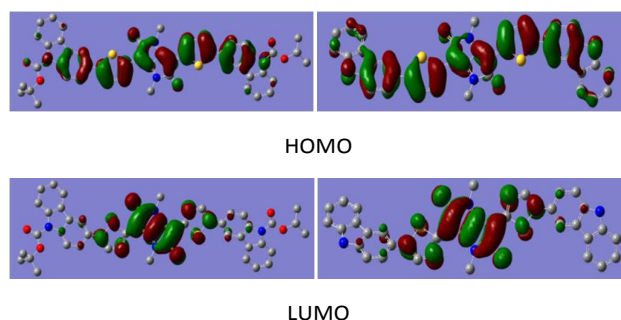
Molecule simulation

HOMO

LUMO

Figure 11 DFT-optimized charge-density isosurfaces of the frontier orbitals for DPP-Car-Boc (left) and DPP-Car (right). The H atoms are omitted for clarity.

To exclude the modification impact of the molecular geometry and electronic structure on absorption property, one DPP unit and two thiophene and carbazole units were selected as repeating units and the molecule simulation was carried out in the ground state. 2-ethylhexyl in DPP unit was replaced with methyl for cost saving. The crucial data and results are listed in Table 2 and Figure 11. After the cleavage of t-butyloxy carbonyl protecting group, the dihedral angles between DPP and thiophene units increase slightly by about 1° while the decreased dihedral angles between carbazole and thiophene plane are observed, but the tiny distortion angle change (1 ~ 2 °) of the backbone is somewhat negligible for the explanation of the absorption broadening effect. As shown in Figure 11, the HOMO spread over the whole backbone, while the LUMO is mainly located in the DPP-thiophene unit for both DPP-Car-Boc and DPP-Car, as the t-butyloxy carbonyl functional group is defined as very weak electron-withdrawing functionality. Cyclic voltammetry is an effective method to determine the redox behavior and energy level for the conjugated molecules. As shown in ESI Figure S21, the conjugated polymers show highly similar redox characteristics before and after the remove of the protected t-Boc groups, thus both the onset of oxidation and reduction potentials and HOMO-LUMO levels (Table 1) stay almost unchanged. Consequently, the leaving of

t-butyloxy carbonyl groups shows little effect on both the LUMO and HOMO energy levels and gaps. Therefore, the observed subtle difference of light-absorption in solution state could be explained and the remarkable red-shift and absorption broadening profile in thin film is not caused by the change of electronic structure but the intensified π-π stacking effect, which is effectively obtained through the cleavage of protecting groups and the liberation of active NH groups.

Conclusions

In summary, we have synthesized a thermo-cleavable narrow band-gap polymer based on diketopyrrolopyrrole (DPP) with alkyl groups and carbazole bearing t-butoxycarbonyl (t-Boc). DPP conjugated polymers with high molecular weight (DPP-Car-Boc-H) exhibited broader absorption coverage than that with low molecular weight (DPP-Car-Boc-L) both in solution and solid state. The absorbing coverage was further extended in thin film after the thermo-labile groups (t-Boc) were removed and N-H groups were liberated to form hydrogen bonds between NH and C=O (amide). FTIR analysis characterized and validated the decomposition of t-butoxycarbonyl protecting groups before and after thermal annealing treatment. The intensified aggregating behavior was confirmed systematically through temperature dependant UV-vis spectra and nonsolvent effect. The π-π stacking inducing enhanced interaction of conjugated polymer chains were further verified through photo-emission spectra, SEM and XRD measurements. The impact of electronic structure change is excluded through the molecule simulation by DFT calculation. The viable method through removing the thermo-labile group and forming hydrogen bonds can effectively strengthen the interaction of polymer chains due to the intensified large π delocalized plane and make conjugated polymer films possess broad solar light response spectrum for the use in photoelectric devices.

Acknowledgements

ARTICLE

Notes and references

1 M. C. Orilall and U. Wiesner. *Chem. Soc. Rev.*, 2011, **40**, 520-535.
2 a) P. M. Beaujuge and J. M. J. Fréchet. *J. Am. Chem. Soc.*, 2011, **133**, 20009-20029; b) L. P. Lu, D. Kabra and R. H. Friend. *Adv. Funct. Mater.*, 2012, **22**, 4165-4171.
3 P. K.-H. Ho, L.-L. Chua, M. Dipankar, X. Gao, D. Qi, A. T.-S. Wee, J.-F. Chang and R. H. Friend. *Adv. Mater.*, 2007, **19**, 215-221.
4 a) C. B. Nielsen, M. Turbiez and I. McCulloch. *Adv. Mater.*, 2013, **25**, 1859-1880; b) M. A. Naik and S. Patil. *J. Polym. Sci., Part A: Polym. Chem.*,2013, **51**, 4241-4260; c) L. Dou, J. You, J. Yang, C.-C. Chen, Y. He, S. Murase,T. Moriarty, K. Emery, G. Li and Y. Yang. *Nature Photon.*, 2012, **6**, 180-185.
5 a) A. B. Tamayo, B. Walker and T.-Q. Nguyen. *J. Phys. Chem. C*, 2008, **112**, 15543-15552; b) D. Chandran and K.-S. Lee. *Macromolecular Research*, 2013, **21**, 272-283.
6 a) J. S. Kim, Y. Park, D. Y. Lee, J. H. Lee, J. H. Park, J. K. Kim and K. Cho. *Adv. Funct. Mater.*, 2010, **20**, 540-545; b) C. L. Chochos and S. A. Choulis. *Progress in Polymer Science*, 2011, **36**,1326-1414; c) R. Noriega, J. Rivnay, K. Vandewal, F. P. V. Koch, N. Stingelin, P. Smith, M. F. Toney and A. Salleo. *Nature Mater.*, 2013, **12**, 1038-1044.
7 a) M. Kuhn, J. Ludwig, T. Marszalek, T. Adermann, W. Pisula, K. Müllen, A. Colsmann and M. Hamburger. *Chem. Mater.*, 2015, **27**, 2678-2686; b) F. Huang, H. Wu and Y. Cao. *Chem. Soc. Rev.*, 2010, **39**, 2500-2521; c) O. Hagemann, M. Bjerring, N. Chr. Nielsen and F. C. Krebs. *Sol. Energy Mater. Sol. Cells*, 2008, **92**, 1327-1335; d) M. H. Petersen, S. A. Gevorgyan and F. C. Krebs. *Macromolecules*, 2008, **41**, 8986-8994; e) F. C. Krebs and K. Norrman. *ACS Appl. Mater. Interfaces*, 2010, **2** , 877-887.
8 a) J. Lee, A-R. Han, J. Hong, J. H. Seo, J. H. Oh and C. Yang. *Adv. Funct. Mater.*, 2012, **22**, 4128-4138; b) S. Chen, B. Sun, W. Hong, Z. Yan, H. Aziz,Y. Meng, J. Hollinger, D. S. Seferosd and Y. Li. *J. Mater. Chem. C*, 2014, **2**, 1683-1690.
9 R. Noriega, J. Rivnay, K. Vandewal, F. P. V. Koch, N. Stingelin, P. Smith, M. F. Toney and A. Salleo. *Nature mater.*, 2013, **12**, 1038-1044.
10 J. S. Zambounis , Z. Hao and A. Iqbal. *Nature*, 1997 , **388** , 131.
11 A. D. Becke. *J. Chem. Phys.*, 1993, **98**, 5648.
12 M. J. Frisch, G. W. Trucks, H. B. Schlegel and et al. Gaussian 03, revision C.02, Gaussian, Inc.: Wallingford, CT, 2004.
13 N. Blouin, A. Michaud, D. Gendron, S. Wakim, E. Blair, R. Neagu-Plesu, M. Bellette, G. Durocher, Y. Tao and M. Leclerc. *J. Am. Chem. Soc.*, 2008, **130**, 732-742.
14 S. Zhang, L. Ye, Q. Wang, Z. Li, X. Guo, L. Huo, H. Fan and J. Hou. *J. Phys. Chem. C*, 2013, **117**, 9550-9557.
15 H. Bronstein, Z. Chen, R. S. Ashraf, W. Zhang, J. Du, J. R. Durrant, P. S.Tuladhar, K. Song, S.E. Watkins, Y. Geerts, M. M. Wienk, R. A. J. Janssen, T. Anthopoulos, H. Sirringhaus, M. Heeney and I. McCulloch. *J. Am. Chem. Soc.*, 2011, **133**, 3272-3275.

16 a) L. Bian, D Yang, L. Yin, J Zhang, W Tang. *Macromol. Chem. Phys.*, 2013, **214**, 2136-2143; b)T. K. An, I. Kang, H.-j. Yun, H. Cha, J. Hwang, S. Park, J. Kim, Y. J. Kim, D. S. Chung, S.-K. Kwon, Y.-H. Kim and C. E. Park. *Adv. Mater.*, 2013, **25**, 7003-7009.
17 M. Tong, S. Cho, J. T. Rogers, K. Schmidt, B. B. Y. Hsu, D. Moses, R. C. Coffin , E. J. Kramer, G. C. Bazan, and A. J. Heeger. *Adv. Funct. Mater.*, 2010, **20**, 3959–3965.
18 a) I. Welterlich and B. Tieke. *Polym. Chem.*, 2013, **4**, 3755–3764; b) A. P. Kulkarni, Christopher J. Tonzola, A. Babel and S. A. Jenekhe. *Chem. Mater.*, 2004, **16**, 4556-4573.
19 a) B. Nketia-Yawson, H.-S. Lee, D. Seo, Y. Yoon, W.-T. Park, K. Kwak, H. J. Son, B.S. Kim Y.-Y. Noh. *Adv. Mater.*, 2015, **27**, 3045-3052; b) S. R. Amrutha and M. Jayakannan. *J. Phys. Chem. B*, 2008, **112**, 1119-1129.
20 S. J. George and A. Ajayaghosh. *Chem. Eur. J.*, 2005, **11**, 3217-3227.
21 a) A. R. Murphy, J. Liu, C. Luscombe, D. Kavulak, J. M. J. Fréchet, R. Joseph Kline and M. D. McGehee. *Chem. Mater.*, 2005, **17**, 4892-4899; b) J. J. Apperloo, R. A. J. Janssen, P. R. L. Malenfant and J. M. J. Fréchet. *J. Am. Chem. Soc.*, 2001, **123**, 6916-6924.
22 X.-F. Zhang, Q. Xi and J. Zhao. *J. Mater. Chem.*, 2010, **20**, 6726–6733.
23 Q. Chu and Y. Pang. *Macromolecules*. 2003, **36**, 4614-4618.
24 G. Zeng, W.-L. Yu, S.-J. Chua and W. Huang. *Macromolecules*, 2002, **35**, 6907-6914.
25 a) S. A. Jenekhe and J. A. Osaheni. *Science*, 1994, **265**, 765-768; b) J. A. Osaheni and S. A. Jenekhe. *Macromolecules*, 1994, **27**, 739-742; b) P.-T. Wu , F. S. Kim and S. A. *Chem. Mater.*, 2011, **23**, 4618-4624; c) S. A. Jenekhe, L. Lu and M. M. Alam. *Macromolecules*, 2001, **34**, 7315-7324.
26 K. Balakrishnan, A. Datar, R. Oitker, H. Chen, J. Zuo and L. Zang. *J. Am. Chem. Soc.*, 2005, **127**, 10496-10497.
27 P. Sonar, G.-M. Ng, T. T. Lin, A. Dodabalapur and Z.-K. Chen. *J. Mater. Chem.*, 2010, **20**, 3626-3636.
28 J. Liu, E. N. Kadnikova, Y. Liu, M. D. McGehee and J. M. J. Fréchet. *J. Am. Chem. Soc.*, 2004, **126**, 9486-9487.
29 a) K. Rahimi, I. Botiz, J. O. Agumba, S. Motamen, N. Stingelinbd and G. Reiter. *RSC Adv.*, 2014, **4**, 11121–11123; b) K. Rahimi, I. Botiz, N. Stingelin, N. Kayunkid, M. Sommer, F. P. V. Koch, H. Nguyen, O. Coulembier, P. Dubois, M. Brinkmann and G. Reiter. *Angew. Chem. Int. Ed.*, 2012, **51**, 11131-11135.
30 L. Ye, S. Zhang, W. Zhao, H. Yao and J. Hou. *Chem. Mater.*, 2014, **26**, 3603-3605.
31 a) T.-J. Ha, P. Sonarb and A. Dodabalapur. *Phys. Chem. Chem. Phys.*, 2013, **15**, 9735-9741; b) P. Sonar, S. P. Singh, Y. Li, Z.-E. Ooi, T.-j. Ha, I.w Wong, M. S. Soha and A. Dodabalapur. *Energy Environ. Sci.*, 2011, **4**, 2288-2296; c) Y. Li, S. P. Singh and P. Sonar. *Adv. Mater.*, 2010, **22**, 4862-4866.
32 Y.-C. Li, K.-B. Chen, H.-L. Chen, C.-S. Hsu, C.-S. Tsao, J.-H. Chen and S.-A. Chen. *Langmuir*, 2006, **22**, 11009-11015.
33 a) X. Liu, L. Guo and Y. Gu. *Polymer*, 2005, **46**, 11949-11957; b) X. Liu, G. Gao, L. Dong, G. Ye and Y. Gu. *Polym. Adv. Technol.*, 2009, **20**, 362-366.
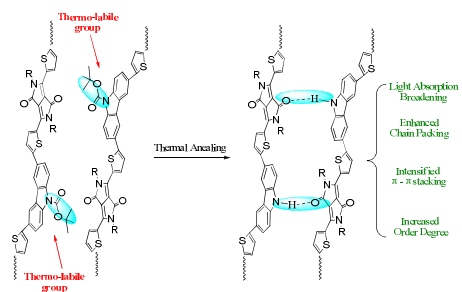
Remove of thermo-labile t-Boc groups in DPP-carbozole copolymer leads to the broadening of light-absorption and increasing of π-π stacking.